

Experimental investigation of concrete-filled cold-formed high strength stainless steel tube columns

Ben Young^{a,*}, Ehab Ellobody^b

^a *Department of Civil Engineering, The University of Hong Kong, Pokfulam Road, Hong Kong*

^b *Department of Structural Engineering, Faculty of Engineering, Tanta University, Tanta, Egypt*

Received 21 February 2005; accepted 16 August 2005

Abstract

This paper presents an experimental investigation of concrete-filled cold-formed high strength stainless steel tube columns. The high strength stainless steel tubes had a yield stress and tensile strength up to 536 and 961 MPa, respectively. The behaviour of the columns was investigated using different concrete cylinder strengths varied from 40 to 80 MPa. A series of tests was performed to investigate the effects of the shape of the stainless steel tube, plate thickness and concrete strength on the behaviour and strength of concrete-filled high strength stainless steel tube columns. The high strength stainless steel tubes were cold-rolled into square and rectangular hollow sections. The depth-to-plate thickness ratio of the tube sections varied from 25.7 for compact sections to 55.8 for relatively slender sections. The columns had different lengths so the length-to-depth ratio generally remained at a constant value of 3. The concrete-filled high strength stainless steel tube specimens were subjected to uniform axial compression. The column strengths, load–axial strain relationships and failure modes of the columns were presented. The test strengths were compared with the design strengths calculated using the American specifications and Australian/New Zealand standards that consider the effect of local buckling using an effective width concept in the calculation of the stainless steel tube column strengths. Based on the test results, design recommendations were proposed for concrete-filled high strength stainless steel tube columns.

© 2005 Elsevier Ltd. All rights reserved.

Keywords: Cold-formed steel; Composite columns; Concrete; Experimental investigation; High strength; Stainless steel tubes; Square hollow sections; Rectangular hollow sections; Structural design

1. Introduction

Concrete-filled steel tube columns provide high strength, high ductility, high stiffness and full usage of construction materials. In addition to these advantages, the steel tubes surrounding the concrete columns eliminate permanent formwork which reduces construction time. Furthermore, the steel tubes assist in carrying axial load as well as providing confinement to the concrete. In recent years, stainless steel tube members have become popular due to the high corrosion resistance, ease of construction and maintenance as well as aesthetic appearance. However, investigation of concrete-filled stainless steel tube columns are rarely found in the literature, especially ones using high strength stainless steel tubes.

Tests of concrete-filled carbon steel tube columns were conducted by Schneider [1], Uy [2–4], Huang et al. [5], Han and

Yao [6], Mursi and Uy [7], Liu et al. [8], Uy [9], Sakino et al. [10], Giakoumelis and Lam [11] and many other researchers. These tests were carried out on concrete-filled carbon mild steel and high strength steel tube columns using circular, square and rectangular hollow sections. To date, no test data are to be found in the literature on concrete-filled stainless steel and high strength stainless steel tube columns. The behaviour of stainless steel sections is different from that of carbon steel sections. Stainless steel sections have a rounded stress–strain curve with no yield plateau and low proportional limit stress compared to carbon steel sections. Recent experimental investigation of stainless steel columns without concrete infilled were conducted by Young and Hartono [12], Young and Liu [13], Liu and Young [14], and Gardner and Nethercot [15,16], while experimental investigations of high strength stainless steel columns were conducted by Young and Lui [17,18].

The local buckling of the steel tube has a considerable effect on the strength and behaviour of concrete-filled steel

* Corresponding author. Tel.: +852 2859 2674; fax: +852 2559 5337.

E-mail address: young@hku.hk (B. Young).

Nomenclature

A_c	Area of concrete
A_e	Effective cross-section area of high strength stainless steel tube
A_s	Full cross-section area of high strength stainless steel tube
B	Overall width of cross-section (smaller dimension)
D	Overall depth of cross-section (larger dimension)
E_o	Initial Young's modulus
E_t	Tangent modulus
f_c	Concrete cylinder strength
F_n	Design stress
F_y	Yield stress ($F_y = \sigma_{0.2}$)
L	Length of column specimen
n	Exponent in Ramberg–Osgood expression
$P_{ACI/ASCE-1}$	Nominal axial strength calculated using the American specifications (unfactored design strength according to approach 1)
$P_{ACI/ASCE-2}$	Nominal axial strength calculated using the American specifications (unfactored design strength according to approach 2)
$P_{ACI/ASCE-3}$	Nominal axial strength calculated using the American specifications (unfactored design strength according to approach 3)
P_{Test}	Test ultimate load (test strength)
r_i	Inside corner radius of stainless steel tube
t	Plate thickness of stainless steel tube
ε_f	Elongation (tensile strain) after fracture based on gauge length of 50 mm
$\sigma_{0.2}$	Static 0.2% proof stress
σ_u	Static ultimate strength

tube columns. Once local buckling has occurred, the steel tube will not be able to provide confinement to the concrete. The column capacity would then be governed by local buckling failure mode. Uy [2] conducted a set of experiments for the local and post-local buckling behaviour of concrete-filled steel box columns, where the steel box sections are considered to be slender sections. A method for determining the required slenderness limits for inelastic local buckling in concrete-filled thin-walled box columns was presented. The results of the investigation were compared with Australian and British standards that consider local buckling of the concrete-filled box columns. It was concluded that the Australian Standard method for determining the post-local buckling behaviour based on the effective width concept for a column under pure compression is suggested for use in an ultimate strength analysis. However, there are no clear guidelines from codes of practice for designing concrete-filled stainless steel tube columns for both slender and non-slender sections. Available design rules for concrete-filled stainless steel tube columns are limited to the general design rules specified in the American specifications [19,20] and Australian standards [21,22] for cold-formed stainless steel and concrete structures.

An experimental investigation was performed in this study to investigate the behaviour and strength of concrete-filled high strength stainless steel tube columns. A series of tests was conducted on square and rectangular hollow sections using different concrete strengths. The columns were subjected to uniform axial compression. The dimensions of the stainless steel tube cross-sections were chosen so that they include both compact and relatively slender sections. The test strengths were compared with the design strengths calculated using the general design rules specified in the American specifications [19,20] and Australian/New Zealand standards [21,22] for stainless steel and concrete structures. The material properties of the stainless steel tubes were obtained using tensile coupon tests and stub column tests.

2. Experimental investigation

2.1. Test specimens

Concrete-filled high strength stainless steel tubes using square hollow sections (SHS) and rectangular hollow sections (RHS) were tested. The tubes were cold-rolled from flat strips of duplex and high strength austenitic stainless steel material. The grade of the duplex stainless steel material is approximately equivalent to EN 1.4462 and UNS S31803. The test programme consisted of five test series that included two series of concrete-filled SHS tubes (SHS1 and SHS2) and three series of concrete-filled RHS tubes (RHS1, RHS2 and RHS3). The nominal section sizes ($D \times B \times t$) of series SHS1, SHS2, RHS1, RHS2 and RHS3 are $150 \times 150 \times 6$, $150 \times 150 \times 3$, $200 \times 110 \times 4$, $160 \times 80 \times 3$ and $140 \times 80 \times 3$ mm, respectively, where D is the overall depth, B is the overall width and t is the plate thickness in mm, as shown in Fig. 1. The measured inner corner radii (r_i) are 5.3, 4.6, 9.1, 6.3 and 7.0 mm for series SHS1, SHS2, RHS1, RHS2 and RHS3, respectively. The measured average overall depth-to-thickness (D/t) ratios are 25.8, 54.1, 48.9, 55.4 and 45.3 for the concrete-filled tube columns of series SHS1, SHS2, RHS1, RHS2 and RHS3, respectively. The lengths (L) are 450, 450, 600, 480 and 420 mm for the concrete-filled tube columns of series SHS1, SHS2, RHS1, RHS2 and RHS3, respectively. The lengths were chosen so that the length-to-depth ratio (L/D) generally remained at a constant value of 3 to prevent overall column buckling. The specimens were tested using nominal concrete cylinder strengths of 40, 60 and 80 MPa. The measured dimensions of the concrete-filled high strength stainless steel tube column test specimens are shown in Table 1.

The concrete-filled high strength stainless steel tube column test specimens are labelled such that the shape of stainless steel tube and concrete strength can be identified from the label. For example, the label “SHS1C40” defines the specimen that has a square hollow section that belonged to test series SHS1, and the letter “C” indicates the concrete strength followed by the value of the concrete strength in MPa (40 MPa). Five tests were conducted on high strength stainless steel tube columns without concrete infilled that are denoted by “C0” in each series.

Table 1
Measured test specimen dimensions

Specimen	Depth D (mm)	Width B (mm)	Thickness t (mm)	D/t	Inner radius r_i (mm)	Length L (mm)	L/D	Stainless steel area A_s (mm ²)	Concrete area A_c (mm ²)
SHS1C0	150.6	150.2	5.855	25.7	5.3	601	4.0	3303	–
SHS1C40	150.5	150.5	5.834	25.8	5.3	450	3.0	3292	19 250
SHS1C60	150.6	150.6	5.829	25.8	5.3	450	3.0	3293	19 281
SHS1C80	150.5	150.5	5.839	25.8	5.3	450	3.0	3296	19 247
SHS2C0	150.5	150.5	2.796	53.8	4.6	600	4.0	1623	–
SHS2C40	150.5	150.5	2.782	54.1	4.6	450	3.0	1615	20 988
SHS2C60	150.5	150.5	2.780	54.1	4.6	450	3.0	1614	20 989
SHS2C80	150.6	150.6	2.780	54.2	4.6	450	3.0	1615	21 018
RHS1C0	196.2	108.5	4.010	48.9	9.1	600	3.0	2303	–
RHS1C40	197.1	109.5	4.060	48.5	9.1	600	3.0	2346	19 088
RHS1C80	197.6	109.6	4.000	49.4	9.1	600	3.0	2317	19 192
RHS2C0	160.1	80.8	2.869	55.8	6.3	600	3.7	1311	–
RHS2C40	160.5	81.3	2.920	55.0	6.3	480	3.0	1339	11 637
RHS2C60	160.7	80.7	2.900	55.4	6.3	480	3.0	1328	11 568
RHS2C80	160.6	80.4	2.900	55.4	6.3	480	3.0	1326	11 514
RHS3C0	140.0	78.8	3.075	45.5	7.0	600	4.3	1263	–
RHS3C40	140.2	80.1	3.100	45.2	7.0	420	3.0	1282	9 861
RHS3C60	140.2	80.1	3.100	45.2	7.0	420	3.0	1282	9 861
RHS3C80	140.3	80.0	3.100	45.3	7.0	420	3.0	1282	9 855

Table 2
Measured material properties obtained from tensile coupon tests for high strength stainless steel tubes

Test series	Section $D \times B \times t$ (mm)	$\sigma_{0.2}$ (MPa)	σ_u (MPa)	E_o (GPa)	ε_f (%)	n
SHS1	$150 \times 150 \times 6$	497	761	194	52	3
SHS2	$150 \times 150 \times 3$	448	699	189	52	4
RHS1	$200 \times 110 \times 4$	503	961	200	36	4
RHS2	$160 \times 80 \times 3$	536	766	208	40	5
RHS3	$140 \times 80 \times 3$	486	736	212	47	6

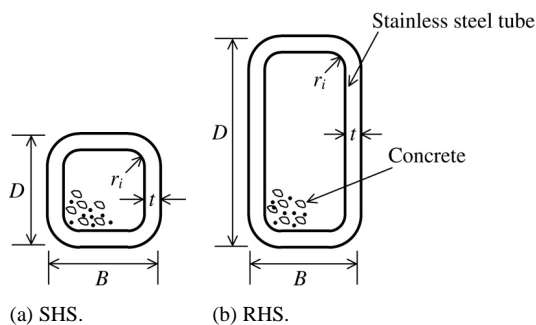


Fig. 1. Definition of symbols for concrete-filled square and rectangular hollow section specimens.

2.2. Material properties of stainless steel tubes

The material properties of the high strength stainless steel tube specimens were determined by tensile coupon tests as well as stub column tests. The tensile coupon test specimens were taken from the centre of the plate at 90° from the weld in the longitudinal direction of the flat portion of the untested specimens. The coupon dimensions conformed to the Australian Standard AS 1391 [23] for the tensile testing of metals using 12.5 mm wide coupons of gauge length 50 mm. The initial Young's modulus (E_o) was measured as 194, 189, 200, 208 and 212 GPa and the measured static 0.2% proof stress

($\sigma_{0.2}$) was 497, 448, 503, 536 and 486 MPa for series SHS1, SHS2, RHS1, RHS2 and RHS3, respectively. The measured elongation after fracture (ε_f) based on a gauge length of 50 mm was 52%, 52%, 36%, 40% and 47% for series SHS1, SHS2, RHS1, RHS2 and RHS3, respectively. The Ramberg–Osgood parameter (n) that describes the shape of the stress–strain curve [24] was 3, 4, 4, 5 and 6 for series SHS1, SHS2, RHS1, RHS2 and RHS3, respectively. The tensile coupon tests of the flat and corner portions are detailed in [17]. Table 2 shows the measured material properties of the flat portion of series SHS1, SHS2, RHS1, RHS2 and RHS3. Figs. 2 and 3 show the complete stress–strain curves obtained from the tensile coupon tests for high strength stainless steel SHS and RHS tubes, respectively.

Five stub column tests of the cold-formed high strength stainless steel SHS and RHS tubes have been conducted to determine the material properties of the complete cross-section. The stub column tests are detailed in [17]. The initial Young's modulus (E_o) was measured as 195, 198, 222, 213 and 214 GPa and the measured static 0.2% proof stress ($\sigma_{0.2}$) was 506, 250, 394, 390 and 441 MPa for series SHS1, SHS2, RHS1, RHS2 and RHS3, respectively. The Ramberg–Osgood parameter (n) was 3, 7, 4, 9 and 6 for series SHS1, SHS2, RHS1, RHS2 and RHS3, respectively. Table 3 shows the measured material properties obtained from the stub column tests for series SHS1,

Table 3

Measured material properties obtained from stub column tests for high strength stainless steel tubes

Test series	Section $D \times B \times t$ (mm)	$\sigma_{0.2}$ (MPa)	σ_u (MPa)	E_o (GPa)	n
SHS1	$150 \times 150 \times 6$	506	570	195	3
SHS2	$150 \times 150 \times 3$	250	254	198	7
RHS1	$200 \times 110 \times 4$	394	418	222	4
RHS2	$160 \times 80 \times 3$	390	411	213	9
RHS3	$140 \times 80 \times 3$	441	444	214	6

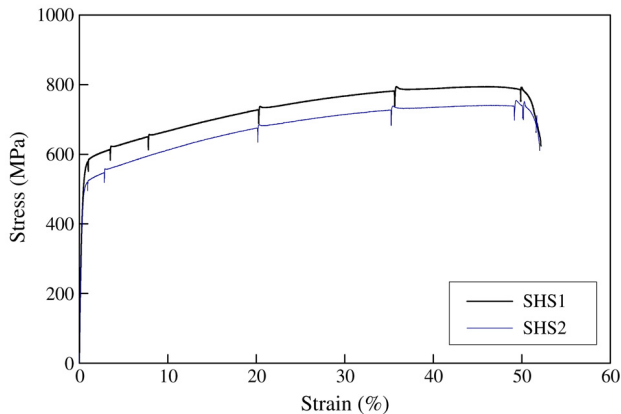


Fig. 2. Complete stress–strain curves obtained from tensile coupon tests for high strength stainless steel SHS tubes.

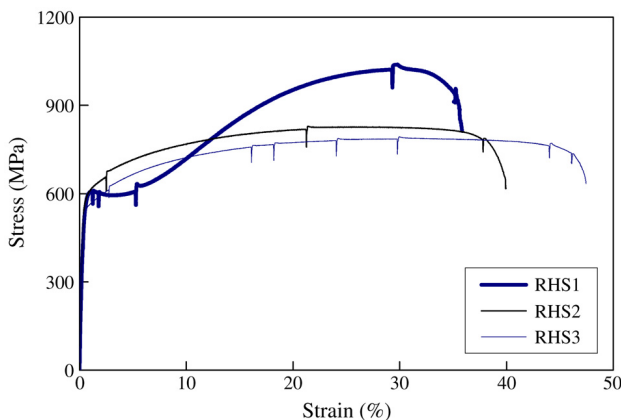


Fig. 3. Complete stress–strain curves obtained from tensile coupon tests for high strength stainless steel RHS tubes.

SHS2, RHS1, RHS2 and RHS3. It should be noted that the values of the 0.2% proof stress ($\sigma_{0.2}$) obtained from the stub column tests are less than those obtained from the tensile coupon tests, except for the $150 \times 150 \times 6$ section. This is due to local buckling that occurred in the stub columns, and lower values of 0.2% proof stress were obtained for the stub column tests.

2.3. Material properties of concrete

The material properties of concrete were determined from standard cylinder tests. The concrete cylinder dimensions and test procedures conformed to the American Specification [20] for concrete testing. The concretes were produced using commercially available materials with normal mixing and curing techniques. The concrete mix design is shown in Table 4.

Twenty-five concrete cylinder tests were conducted. The mean compressive cylinder strengths of the concrete at the time of the concrete-filled stainless steel tube column tests were determined as 46.6, 61.9 and 83.5 MPa with the corresponding coefficients of variation (COV) of 0.045, 0.111 and 0.026 for nominal concrete cylinder strengths of C40, C60 and C80, respectively. Table 5 summarizes the measured concrete cylinder strengths and the number of tests.

2.4. Instrumentation

Three transducers (LVDTs) were used to measure the axial shortening of the columns, as shown in Figs. 4 and 5. The axial shortening was obtained from the average readings of the LVDTs for each column specimen. Seven strain gauges on one side and two strain gauges on the opposite side of the columns were used to monitor the axial strain and plate deformation of each specimen, as shown in Fig. 5. All strain gauges were placed on the outside surface of the high strength stainless steel tubes. The top and bottom gauges were located at a distance of 35 mm from both ends of the columns. The middle strain gauges were positioned at mid-height of each column, equally spaced in line on one face of the columns. A data acquisition system was used to record the LVDTs and strain gauge and applied load readings at regular intervals during the tests.

2.5. Column testing procedure

The concrete-filled high strength stainless steel tube column tests are shown in Fig. 4. A 4600 kN capacity 815 Rock Mechanics Test System servo-controlled hydraulic testing machine was used to apply compressive axial force to the column specimens. Prior to testing, both ends of the columns were strengthened by steel brackets so that failure would not occur at the ends and the column strength would not be influenced by end effects. The ends of the columns were cast in plaster with large thicknesses of rigid steel plates being used. The load was applied to the columns in axial uniform compression over the concrete and steel tube, as shown in Fig. 4. The values of the longitudinal strain gauges near the four corners of the columns were checked carefully while loading was applied to the columns within the elastic limit. This is to ensure that the load was applied concentrically to the columns. Displacement control was used to drive the hydraulic actuator at a constant speed of 0.5 mm/min. This allowed the tests to be continued in the post-ultimate range.

Table 4
Concrete mix design

Nominal concrete strength (MPa)	Water/cement ratio	Mix proportions (to the weight of cement)					
		Cement	Water	Fine aggregate	Coarse aggregate	Fly ash	Super-plasticizer
C40	0.74	1.0	0.74	2.96	3.95	0.36	0
C60	0.41	1.0	0.41	1.12	2.25	0.0	0
C80	0.28	1.0	0.28	1.20	1.80	0.0	0.01

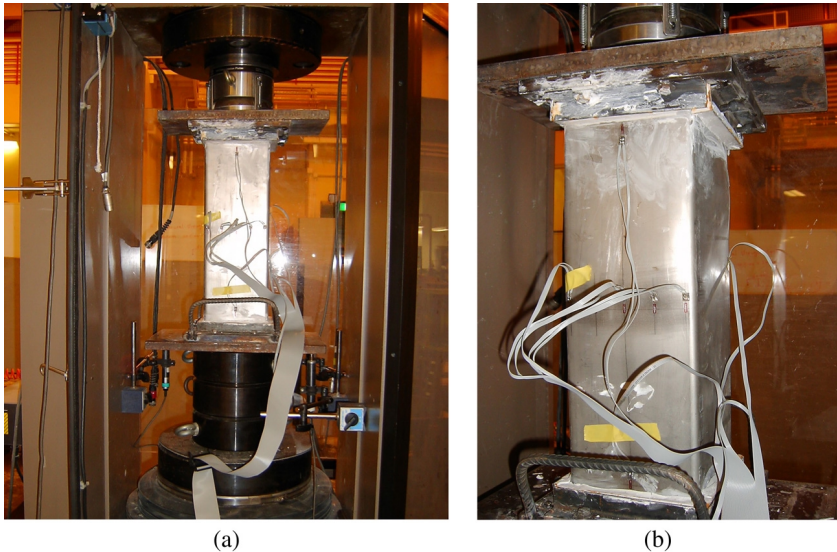


Fig. 4. Test set-up of concrete-filled stainless steel tube specimens.

Table 5
Measured concrete cylinder strengths

Nominal concrete strength (MPa)	Mean value of measured concrete strength (MPa)	Coefficient of variation COV	Number of concrete cylinder tests
C40	46.6	0.045	10
C60	61.9	0.111	9
C80	83.5	0.026	6

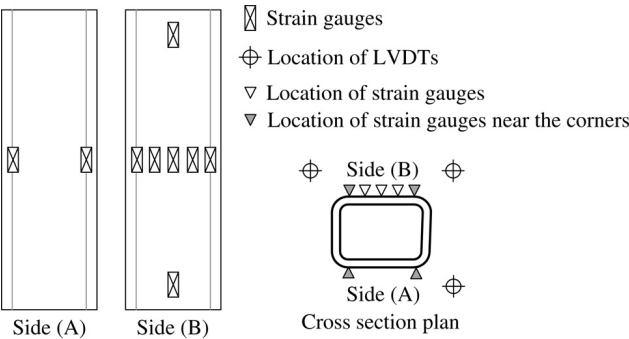


Fig. 5. Location of strain gauges and LVDTs on the specimens.

3. Test results

The test strengths and load–axial strain relationships were measured for each column specimen. The test strengths (P_{Test}) of the concrete-filled high strength stainless steel tube columns of the SHS and RHS are shown in Tables 6 and 7, respectively.

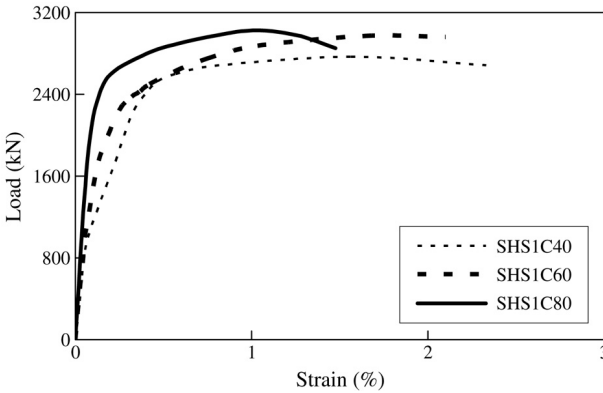


Fig. 6. Load versus average strain curves for concrete-filled specimens of series SHS1.

The load–axial strain relationships of the concrete-filled tube columns for series SHS1 are shown in Fig. 6. The average strains near the four corners of the columns were plotted. It can be seen that the ductility of the columns generally decreases with increase of the concrete strength.

Generally the local buckling failure mode of the high strength stainless steel tubes was observed for specimens with relatively slender sections for series SHS2, RHS1, RHS2 and RHS3. A concrete crushing failure mode together with local buckling of the high strength stainless steel tubes for specimens with compact sections for series SHS1 was also observed. The failure mode of column specimen SHS1C60 having a square hollow section of nominal dimensions $150 \times 150 \times 6$ mm

Table 6
Test strengths and design strengths of concrete-filled square hollow section columns

Specimen	P_{Test} (kN)	$P_{ACI/ASCE-1}$ (kN)	$P_{ACI/ASCE-2}$ (kN)	$P_{ACI/ASCE-3}$ (kN)	$\frac{P_{Test}}{P_{ACI/ASCE-1}}$	$\frac{P_{Test}}{P_{ACI/ASCE-2}}$	$\frac{P_{Test}}{P_{ACI/ASCE-3}}$
SHS1C0	1927.4	1641.4	1671.1	1927.4	1.17	1.15	1.00
SHS1C40	2768.1	2399.4	2429.1	2689.9	1.15	1.14	1.03
SHS1C60	2972.0	2651.2	2680.9	2941.9	1.12	1.11	1.01
SHS1C80	3019.9	3004.4	3034.0	3293.5	1.01	1.00	0.92
SHS2C0	408.6	497.4	343.2	408.6	0.82	1.19	1.00
SHS2C40	1381.5	1324.5	1171.7	1239.9	1.04	1.18	1.11
SHS2C60	1620.0	1596.9	1444.3	1512.9	1.01	1.12	1.07
SHS2C80	1851.3	1984.4	1831.8	1900.4	0.93	1.01	0.97
Mean	–	–	–	–	1.03	1.11	1.01
COV	–	–	–	–	0.114	0.064	0.058

Table 7
Test strengths and design strengths of concrete-filled rectangular hollow section columns

Specimen	P_{Test} (kN)	$P_{ACI/ASCE-1}$ (kN)	$P_{ACI/ASCE-2}$ (kN)	$P_{ACI/ASCE-3}$ (kN)	$\frac{P_{Test}}{P_{ACI/ASCE-1}}$	$\frac{P_{Test}}{P_{ACI/ASCE-2}}$	$\frac{P_{Test}}{P_{ACI/ASCE-3}}$
RHS1C0	957.0	965.2	808.1	957.0	0.99	1.18	1.00
RHS1C40	1627.2	1742.6	1581.9	1713.1	0.93	1.03	0.95
RHS1C80	2180.0	2329.5	2172.1	2319.2	0.94	1.00	0.94
RHS2C0	537.3	542.2	423.0	537.3	0.99	1.27	1.00
RHS2C40	881.5	1018.3	895.7	998.2	0.87	0.98	0.88
RHS2C60	1014.5	1159.0	1038.0	1146.0	0.88	0.98	0.89
RHS2C80	1280.1	1366.6	1245.9	1354.5	0.94	1.03	0.95
RHS3C0	558.2	538.6	498.5	558.2	1.04	1.12	1.00
RHS3C40	1048.7	939.2	898.3	948.8	1.12	1.17	1.11
RHS3C60	1096.9	1067.4	1026.5	1077.0	1.03	1.07	1.02
RHS3C80	1258.8	1247.8	1206.9	1257.7	1.01	1.04	1.00
Mean	–	–	–	–	0.98	1.08	0.98
COV	–	–	–	–	0.076	0.087	0.066



Fig. 7. Failure mode of column specimen SHS1C60.

and nominal concrete cylinder strength of 60 MPa is shown in Fig. 7. For this specimen, concrete crushing as well as local buckling of the high strength stainless steel tube were observed. The failure mode of column specimen RHS2C40 having a rectangular hollow section of nominal dimensions



(a) Elevation. (b) Side view.

Fig. 8. Failure mode of column specimen RHS2C40.

160 × 80 × 3 mm and a nominal concrete cylinder strength of 40 MPa is shown in elevation and side view in Fig. 8. It is shown that local buckling dominated the failure of the column.

4. Design rules

4.1. General

The concrete-filled cold-formed high strength stainless steel tube column test strengths (P_{Test}) are compared with the unfactored design strengths predicted using the general guidelines specified in the American specifications [19,20] and Australian/New Zealand standards [21,22] for cold-formed stainless steel and concrete structures. These specifications consider the effect of local buckling of stainless steel tubes using the effective width concept in the calculation of the design strengths. The American specifications and Australian/New Zealand standards for cold-formed stainless steel and concrete structures generally use the same formula to calculate the design strengths. The design strengths ($P_{\text{ACI/ASCE}}$) for the concrete-filled stainless steel tube columns were obtained by determining the strength of the stainless steel tube ($A_e F_n$) using the specifications [19,21] for cold-formed stainless steel structures as well as the strength of the concrete infilled ($0.85A_c f_c$) using the specifications [20,22] of the concrete structures, as shown in Eq. (1):

$$P_{\text{ACI/ASCE}} = A_e F_n + 0.85A_c f_c \quad (1)$$

where A_e is the effective cross-section area of the stainless steel tube that is equal to the full cross-section area (A_s) in the case of compact cross-sections and less than A_s in the case of slender cross-sections due to the effect of local buckling, F_n is the flexural buckling stress determined according to Sections 3.4.1 and 3.4.2 of the American Specification [19] and the Australian/New Zealand Standard [21], respectively, A_c is the area of concrete and f_c is the measured concrete cylinder strength. In the calculation of the strength of the stainless steel tubes, it was found that the values of the design stresses (F_n) are equal to the yield stresses (F_y) for all columns. This is due to the short column lengths. In this study, the yield stress (F_y) is taken as the measured static 0.2% proof stress ($\sigma_{0.2}$).

The American and Australian/New Zealand specifications use the same Winter effective width equations in calculating the effective area (A_e) of stainless steel tube cross-sections. In the calculation of buckling stress (F_n), the design rules specified in the American Specification are based on the Euler column strength that requires the calculation of the tangent modulus (E_t) using an iterative design procedure. The design rules specified in the Australian Standard adopt the Euler column strength or alternatively the Perry curve that needs only the initial Young's modulus (E_o) and a number of parameters to calculate the design stress. In this study, the Euler column strength method is used in the calculation of the design strengths for the Australian/New Zealand Standard. Hence, the design strengths calculated using Eq. (1) are identical for the American and Australian/New Zealand specifications. The columns were designed as concentrically loaded compression members. The term $0.85A_c f_c$ in Eq. (1) represents the contribution of the concrete infilled in the calculation of the column design strengths.

Three design approaches were investigated in the calculation of the column design strengths using Eq. (1). The calculated unfactored design strengths are denoted by $P_{\text{ACI/ASCE-1}}$, $P_{\text{ACI/ASCE-2}}$ and $P_{\text{ACI/ASCE-3}}$. The three design approaches are shown in the following sections.

4.2. Design approach 1 ($P_{\text{ACI/ASCE-1}}$)

The design strengths ($P_{\text{ACI/ASCE-1}}$) are calculated using the material properties obtained from the tensile coupon tests for high strength stainless steel tubes in the calculation of the term $A_e F_n$ in Eq. (1). The measured material properties obtained from the tensile coupon tests are tabulated in Table 2. The calculation of the strength of the concrete infilled for the term $0.85A_c f_c$ in Eq. (1) is carried out using the measured concrete cylinder strengths tabulated in Table 5.

4.3. Design approach 2 ($P_{\text{ACI/ASCE-2}}$)

In this approach, the calculation of the term $A_e F_n$ in Eq. (1) is carried out using the material properties obtained from the stub column tests for high strength stainless steel tubes. The measured material properties obtained from the stub column tests are tabulated in Table 3. The design strengths calculated from Eq. (1) in this case are denoted by $P_{\text{ACI/ASCE-2}}$. The strength of the concrete infilled is calculated in the same way as with design approach 1.

4.4. Design approach 3 ($P_{\text{ACI/ASCE-3}}$)

In this approach, the term $A_e F_n$ in Eq. (1) is replaced by the test strengths of the high strength stainless steel tubes without concrete infilled for each series of test. Hence, the strengths of the high strength stainless steel tubes are 1927.4, 408.6, 957.0, 537.3, and 558.2 kN for series SHS1, SHS2, RHS1, RHS2 and RHS3, respectively. Once again, the strength of the concrete infilled is calculated in the same way as with design approach 1. The design strengths calculated from Eq. (1) in this case are denoted by $P_{\text{ACI/ASCE-3}}$.

5. Comparison of test strengths with design strengths

The comparison of test strengths (P_{Test}) with design strengths ($P_{\text{ACI/ASCE-1}}$, $P_{\text{ACI/ASCE-2}}$ and $P_{\text{ACI/ASCE-3}}$) is shown in Tables 6 and 7 for the concrete-filled high strength stainless steel tube columns of SHS and RHS specimens, respectively. The mean values of the $P_{\text{Test}}/P_{\text{ACI/ASCE-1}}$, $P_{\text{Test}}/P_{\text{ACI/ASCE-2}}$ and $P_{\text{Test}}/P_{\text{ACI/ASCE-3}}$ ratios are 1.03, 1.11 and 1.01 with the corresponding coefficients of variation (COV) of 0.114, 0.064 and 0.058 for the SHS columns, as shown in Table 6. The mean values of the $P_{\text{Test}}/P_{\text{ACI/ASCE-1}}$, $P_{\text{Test}}/P_{\text{ACI/ASCE-2}}$ and $P_{\text{Test}}/P_{\text{ACI/ASCE-3}}$ ratios are 0.98, 1.08 and 0.98 with the corresponding COV of 0.076, 0.087 and 0.066 for the RHS columns, as shown in Table 7.

The test strengths (P_{Test}) and the design strengths ($P_{\text{ACI/ASCE-1}}$, $P_{\text{ACI/ASCE-2}}$ and $P_{\text{ACI/ASCE-3}}$) were plotted against the measured concrete strengths, as shown in Figs. 9–13. The column strengths are shown on the vertical axis

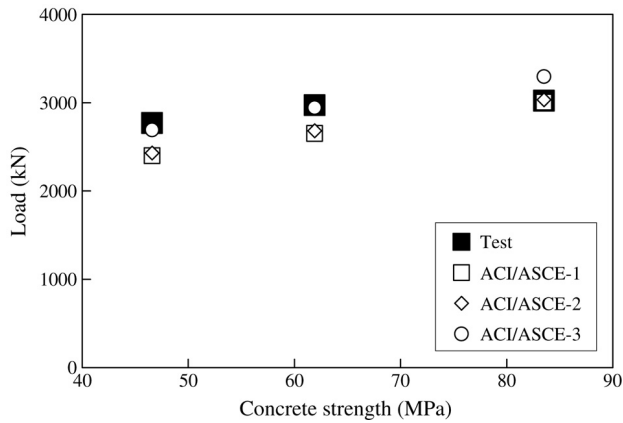


Fig. 9. Comparison of test strengths with design strengths for concrete-filled specimens of series SHS1.

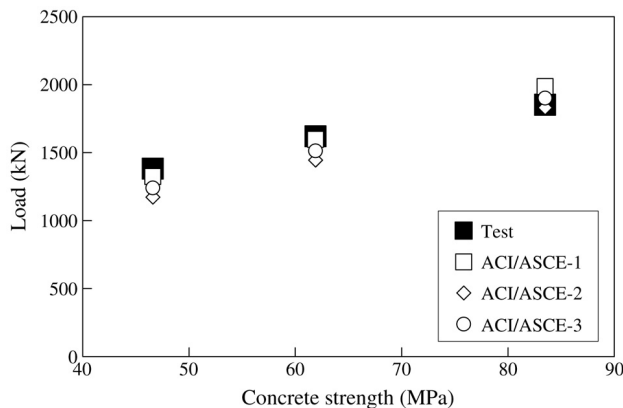


Fig. 10. Comparison of test strengths with design strengths for concrete-filled specimens of series SHS2.

of Figs. 9–13, while the measured concrete cylinder strengths are shown on the horizontal axis. Fig. 9 shows the comparison of the test strengths with the design strengths for concrete-filled high strength stainless steel compact section tube columns of series SHS1. It can be seen that $P_{ACI/ASCE-1}$ and $P_{ACI/ASCE-2}$ are conservative for the columns having nominal concrete cylinder strengths of 40 and 60 MPa, and accurately predicted the strength of the column having the nominal concrete cylinder strength of 80 MPa. It is shown that $P_{ACI/ASCE-3}$ accurately predicted the test strengths of the columns having nominal concrete cylinder strengths of 40 and 60 MPa, but overestimated the strength of the column having the nominal concrete cylinder strength of 80 MPa.

Figs. 10–13 show the comparison of the test strengths with the design strengths for concrete-filled high strength stainless steel relative to slender section tube columns of series SHS2, RHS1, RHS2 and RHS3. It can be seen that $P_{ACI/ASCE-1}$ and $P_{ACI/ASCE-3}$ are unconservative for most of the columns having nominal concrete cylinder strengths of 40, 60 and 80 MPa, except for the columns SHS2C40, SHS2C60 and the columns in series RHS3. On the other hand, the design strengths $P_{ACI/ASCE-2}$ that use the material properties obtained from the stub column tests in the calculation of the strengths of the stainless steel tubes are conservative for most of the columns for the three concrete strengths, except for the columns RHS2C40

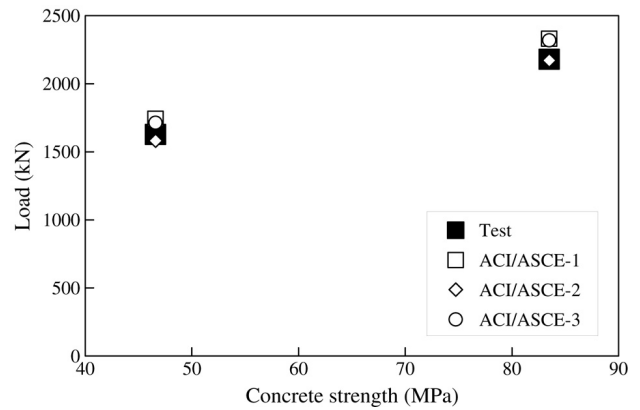


Fig. 11. Comparison of test strengths with design strengths for concrete-filled specimens of series RHS1.

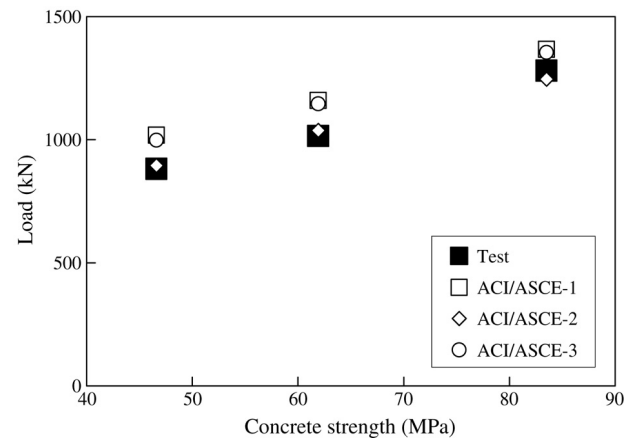


Fig. 12. Comparison of test strengths with design strengths for concrete-filled specimens of series RHS2.

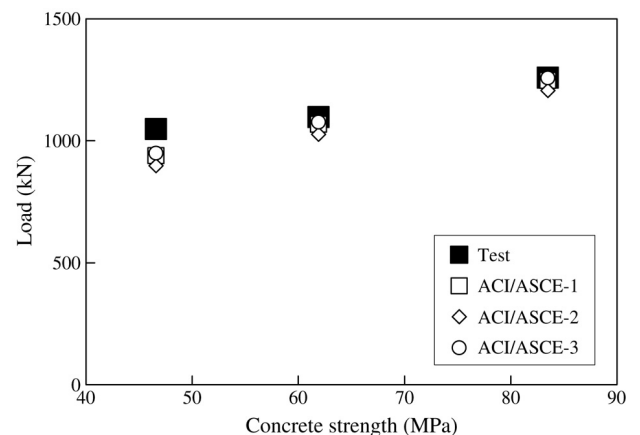


Fig. 13. Comparison of test strengths with design strengths for concrete-filled specimens of series RHS3.

and RHS2C60, for which they are slightly unconservative. Hence, it is recommended that the material properties obtained from stub column tests are used in the calculation of the design strengths for concrete-filled high strength stainless steel tube columns.

6. Conclusions

An experimental investigation of concrete-filled cold-formed high strength stainless steel tube columns has been presented in this paper. Tests on concrete-filled high strength stainless steel square and rectangular hollow section columns which were concentrically loaded were carried out. The overall depth-to-plate thickness ratio of the tube sections varied from 25.7 for compact sections to 55.8 for relatively slender sections. Different concrete cylinder strengths varying from 40 to 80 MPa were investigated. The column strengths, load–axial strain relationships and failure modes of the columns have been reported.

The test strengths were compared with the design strengths predicted using the American and Australian/New Zealand specifications for cold-formed stainless steel and concrete structures. The material properties of the high strength stainless steel tube specimens obtained from tensile coupon tests and stub column tests were used to calculate the design strengths. The test strengths of the high strength stainless steel tubes without concrete infilled were also used to calculate the design strengths. It is shown that the design strengths calculated using the material properties of stainless steel obtained from the tensile coupon tests as well as the test strengths of the high strength stainless steel tubes without concrete infilled are generally unconservative for the concrete-filled stainless steel tube columns tested. It is demonstrated that the design strengths calculated using the material properties of stainless steel obtained from the stub column tests are generally conservative for both compact and slender sections with different concrete strengths. Therefore, it is recommended that the design rules in the American and Australian/New Zealand specifications for cold-formed stainless steel and concrete structures are used for the design of concrete-filled cold-formed high strength stainless steel tube columns provided that the design strengths are calculated using the material properties of stainless steel obtained from stub column tests.

Acknowledgments

The authors are grateful to STALA Tube Finland for supplying the test specimens. The authors are also grateful to Mr. Kin-Chung Tsang and King-Hung Poon for their assistance in this project.

References

- [1] Schneider SP. Axially loaded concrete-filled steel tubes. *Journal of Structural Engineering*, ASCE 1998;124(10):1125–38.

- [2] Uy B. Local and post-local buckling of concrete filled steel welded box columns. *Journal of Constructional Steel Research* 1998;74(1–2):47–72.
- [3] Uy B. Static long-term effects in short concrete-filled steel box columns under sustained loading. *ACI Structural Journal* 2001;98(1):96–104.
- [4] Uy B. Strength of short concrete filled high strength steel box columns. *Journal of Constructional Steel Research* 2001;57(2):113–34.
- [5] Huang CS, Yeh YK, Hu HT, Tsai KC, Weng YT, Wang SH et al. Axial load behavior of stiffened concrete-filled steel columns. *Journal of Structural Engineering*, ASCE 2002;128(9):1222–30.
- [6] Han LH, Yao GH. Influence of concrete compaction on the strength of concrete-filled steel RHS columns. *Journal of Constructional Steel Research* 2003;59(6):751–67.
- [7] Mursi M, Uy B. Strength of concrete filled steel box columns incorporating interaction buckling. *Journal of Structural Engineering*, ASCE 2003;129(5):626–39.
- [8] Liu D, Gho WM, Yuan J. Ultimate capacity of high-strength rectangular concrete-filled steel hollow section stub columns. *Journal of Constructional Steel Research* 2003;59(12):1499–515.
- [9] Uy B. High-strength steel–concrete composite columns for buildings. *Structures & Buildings* 2003;156:3–14.
- [10] Sakino K, Nakahara H, Morino S, Nishiyama I. Behavior of centrally loaded concrete-filled steel-tube short columns. *Journal of Structural Engineering*, ASCE 2004;130(2):180–8.
- [11] Giakoumelis G, Lam D. Axial capacity of circular concrete-filled tube columns. *Journal of Constructional Steel Research* 2004;60(7):1049–68.
- [12] Young B, Hartono W. Compression tests of stainless steel tubular members. *Journal of Structural Engineering*, ASCE 2002;128(6):754–61.
- [13] Young B, Liu Y. Experimental investigation of cold-formed stainless steel columns. *Journal of Structural Engineering*, ASCE 2003;129(2):169–76.
- [14] Liu Y, Young B. Buckling of stainless steel square hollow section compression members. *Journal of Constructional Steel Research* 2003;59(2):165–77.
- [15] Gardner L, Nethercot DA. Experiments on stainless steel hollow sections—Part 1: Material and cross-sectional behaviour. *Journal of Constructional Steel Research* 2004;60:1291–318.
- [16] Gardner L, Nethercot DA. Experiments on stainless steel hollow sections—Part 2: Member behaviour of columns and beams. *Journal of Constructional Steel Research* 2004;60:1319–32.
- [17] Young B, Lui WM. Behaviour of cold-formed high strength stainless steel sections. *Journal of Structural Engineering*, ASCE 2005;131(11).
- [18] Young B, Lui WM. Experimental investigation of cold-formed high strength stainless steel compression members. In: *Proceedings of the 6th international conference on tall buildings*. 2005.
- [19] ASCE. Specification for the design of cold-formed stainless steel structural members. SEI/ASCE-8-02. Reston (VA): American Society of Civil Engineers; 2002.
- [20] ACI. Building code requirements for structural concrete and commentary. ACI 318-95. Detroit (USA): American Concrete Institute; 1995.
- [21] AS/NZS. Cold-formed stainless steel structures. Australian/New Zealand Standard, AS/NZS 4673:2001. Sydney (Australia): Standards Australia; 2001.
- [22] Australian Standards AS3600. Concrete structures. AS3600-1994. Sydney (Australia): Standards Australia; 1994.
- [23] AS. Methods for tensile testing of metals. Australian Standard, AS 1391 – 1991. Sydney (Australia): Standards Association of Australia; 1991.
- [24] Ramberg W, Osgood WR. Description of stress strain curves by three parameters. Technical note no. 902. Washington (DC): National Advisory committee for Aeronautics; 1943.